Issues in the application of Suspension-Point Interferometer to Advanced LIGO

Yoichi Aso / Columbia University
LIGO-T070209-00-Z

August 29, 2007

Revision history

- Jun 13 2007: Initial version
- Aug. 24 2007: Revised

1 Introduction

Through recent study of the lock acquisition scheme for Advanced LIGO, it was realized that the RMS speed of the test mass mirrors has to be further reduced at least by a factor of 10 or preferably 100 from the current requirement of the seismic isolation [1]. A possible solution to this problem is suspension point interferometer (SPI). SPI is an auxiliary interferometer which monitors the distance between the suspension points of the input and end test masses. By the servo control to keep the SPI in resonance, the differential motion of the test mass suspension points is suppressed by a large factor. Thus a good common mode rejection can be expected even with the arm cavity length of 4 km.

Recently (July, 2007), the ANU group proposed an alternative approach for robust lock acquisition called "Lock Acquisition Interferometer" or LAI [7]. LAI is defined, at least in this document, as an interferometer which is co-located with the main interferometer and used for lock acquisition by sensing the same degrees of freedom as the main interferometer with much wider sensing range. Although the study has just started, the LAI concept looks like very promising. Now if the LAI is employed in advanced LIGO, SPI will not be necessary for lock acquisition purpose. However, there are other advantages in SPI which are not available with LAI. Therefore, an issue to be addressed here is whether to use SPI in combination with LAI or not.

In this document, I will discuss the possibility of implementing SPI in advanced LIGO and try to provide information to serve as a basis for the decision of whether to use SPI or not.

2 Principle of the SPI

The working principle of SPI is shown by conceptual drawings in Fig.1. In this case, an auxiliary interferometer is formed by the penultimate masses[1] above the main interferometer (MIF). Once the SPI is

[1] This is not a requirement for SPI. The auxiliary interferometer could be placed anywhere above the main interferometer depending on the choice of practical implementation.

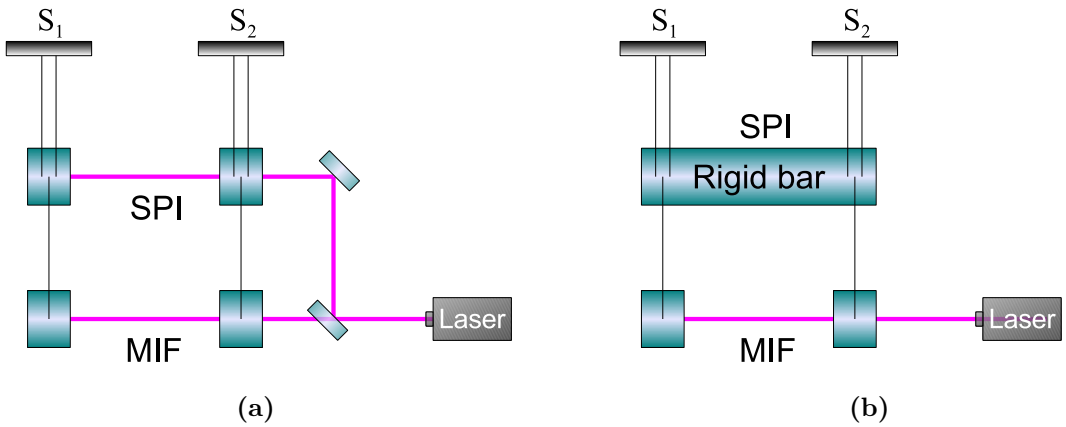

Fig. 1: Working principle of SPI.

locked, the differential motion of the mirrors of the SPI is suppressed to the accuracy of the servo loop. Therefore, the SPI can be considered as a rigid bar hung across the two suspension systems (Fig.1 (b)). If the pendulums hanging from this virtual rigid bar are identical, no differential motion will be transmitted to the MIF. Consequently the seismic noise in the MIF is significantly reduced. However in reality, the pendulums are not exactly identical. A fraction of the common motion at the SPI stage is converted to differential motion at the MIF by asymmetry of the suspensions.

As a measure of this effect, I define the common mode rejection ratio (CMRR) of SPI as:

$$\mathrm{CMRR} \equiv 2\left|\frac{H_1(\omega) - H_2(\omega)}{H_1(\omega) + H_2(\omega)}\right| \tag{1}$$

Here $H_1(\omega)$ and $H_2(\omega)$ are the transfer functions of the suspensions hanging below the SPI stage. In the case of single pendulums as shown in Fig.1 (b), the CMRR is approximately written as,

$$\mathrm{CMRR} \simeq |H_1(\omega)| \sqrt{\left(\frac{\Delta l}{g}\right)^2 \omega^4 + \left(\frac{l\gamma}{mg}\right)^2 \left(\frac{\Delta l}{l} + \frac{\Delta\gamma}{\gamma} - \frac{\Delta m}{m}\right)^2 \omega^2}. \tag{2}$$

$$H_1(\omega) \equiv \frac{1}{1 + i\frac{l\gamma}{mg}\omega - \frac{l}{g}\omega^2}, \tag{3}$$

where l, m, γ are the length, mass and damping factor of the pendulum 1 and the letters with Δ represent the difference between the corresponding parameters of the two pendulums [4]. The frequency dependence of CMRR is plotted in Fig.2 in the case of 1% asymmetry. At frequencies higher than the resonance of the pendulum, the CMRR approaches to a plateau at $1/(\omega_1 - \omega_2)^2$, where ω_1 and ω_2 are the resonant frequencies of the pendulums. At lower frequencies the CMRR improves dramatically as the frequency goes down. The CMRR is poor at the resonant frequency. In the case of multiple pendulums, the shape of the CMRR around the resonances changes but the general trend is the same.

CMRR is one of the limiting factors of the performance of an SPI. Other limiting factors includes coupling from other degrees of freedom, servo gain of the SPI, noise of the SPI and so on. Detailed discussion on those factors can be found in [4].

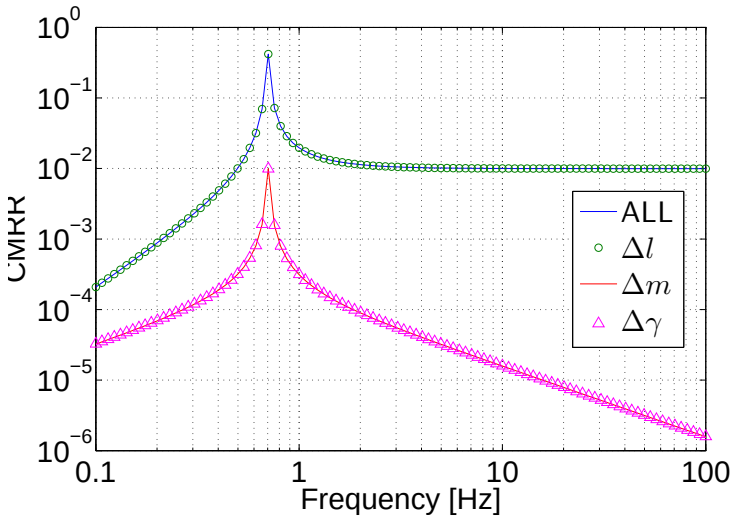

Fig. 2: Frequency dependence of CMRR: The blue line shows the CMRR with all asymmetries included. The green circles show the CMRR with only Δl. The red line is the CMRR with only Δm. The pink triangles show the CMRR with only $\Delta\gamma$. All asymmetries are 1%.

3 Past studies

Originally, suspension point interferometer was proposed by Drever [5] about 20 years ago as a part of the LIGO vibration isolation system. Although it was not included in the final LIGO design, he tested this idea with an asymmetric Michelson interferometer [6]. Independently in Japan I conducted several experiments and demonstrated the effectiveness of SPI using Fabry-Perot interferometers [2, 3, 4]. In this section, I will summarize the latest results from my experiment. For details, refer to [4].

3.1 Experimental Setup

The experimental setup is shown in Fig.3. It is basically 1.5 m long Fabry-Perot interferometers suspended as triple pendulums. A rigid ring-cavity mode cleaner is used for frequency stabilization and spatial filtering of the laser.

The triple pendulum suspension system for the test masses incorporates two monolithic geometric anti-spring filters (MGAS filters) at first and second stages for vertical vibration isolation. Eddy current damping is applied to the first stage of the suspension to take away the energy from the pendulum swiftly. The second stages form an SPI and the final stage the main interferometer. The final mirror is surrounded by a recoil mass and actuated by coil-magnet actuators from the recoil mass.

3.2 Results

Two noise spectra of the MIF are shown in Fig.5. The blue curve was measured when the SPI is not used and the red was taken with the SPI turned on. At frequencies below the resonances of the suspension,

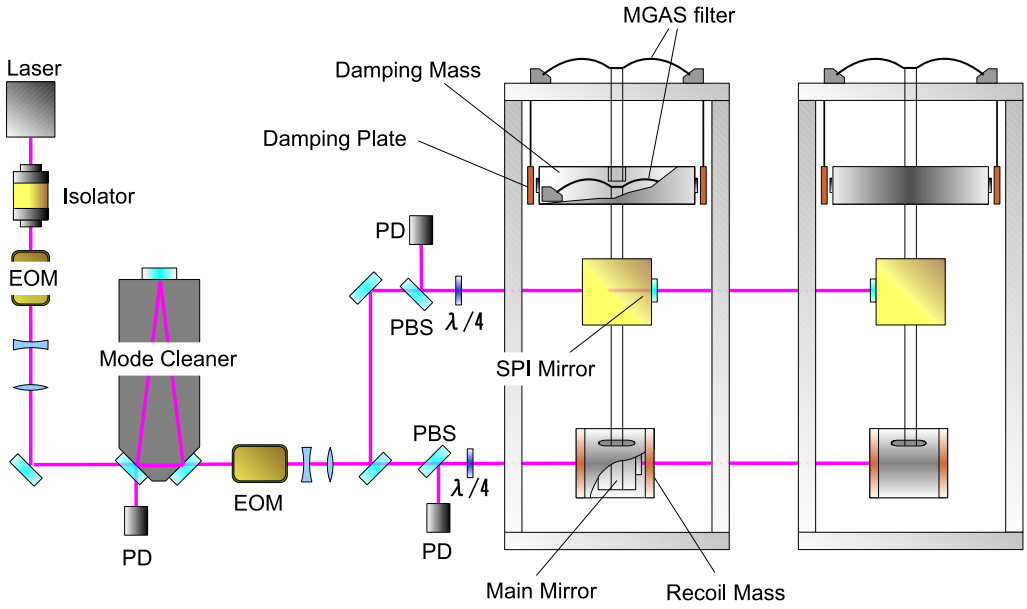

Fig. 3: The overview of the experimental setup.

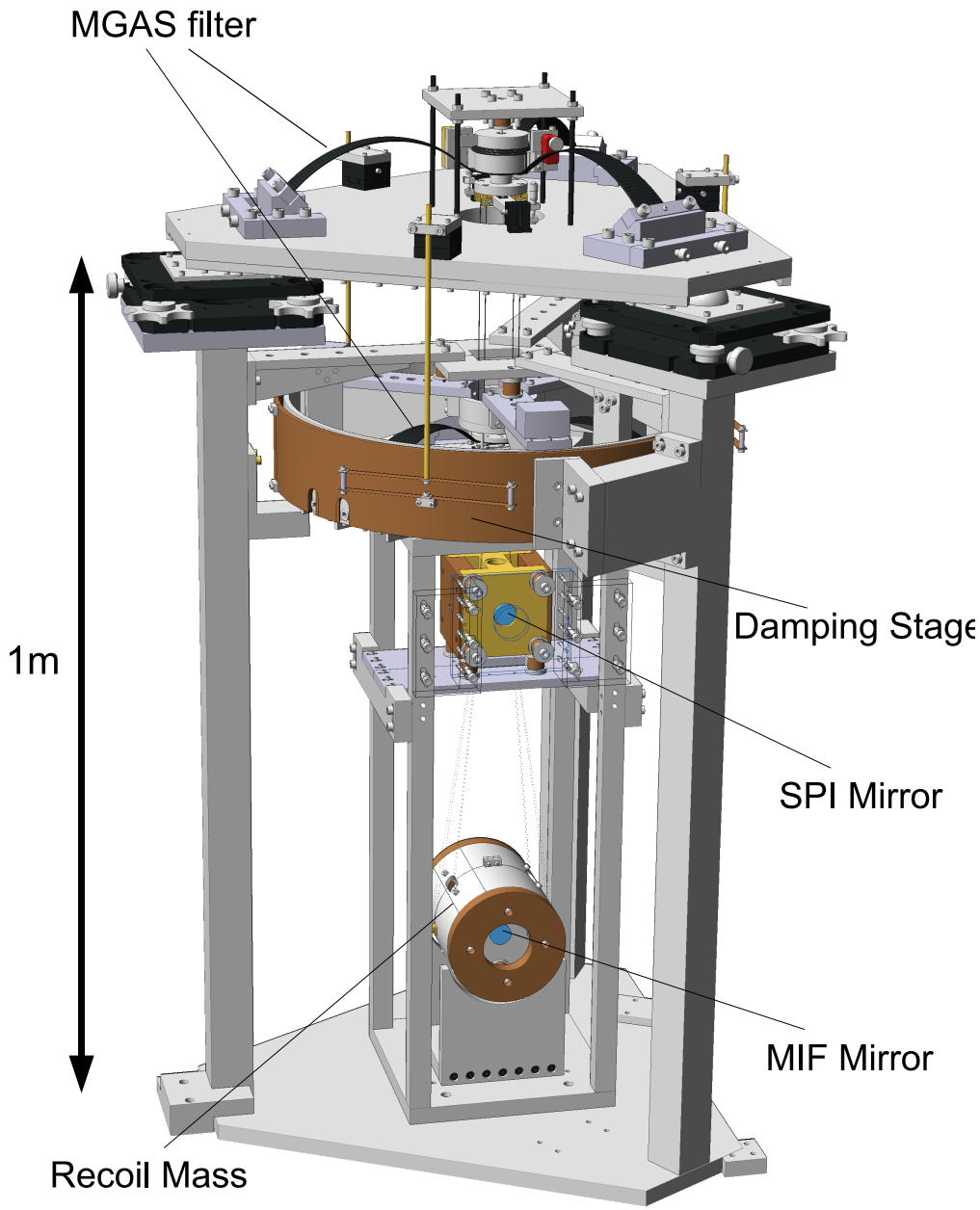

Fig. 4: Suspension system.

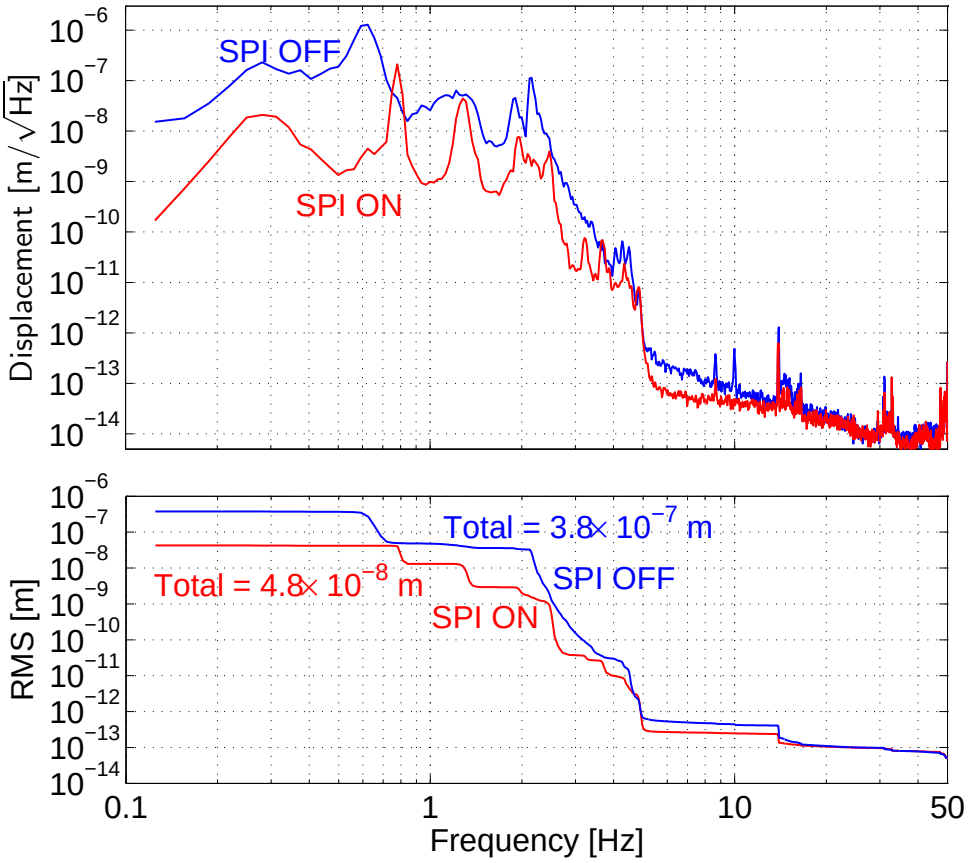

Fig. 5: Displacement noise spectra of the MIF. The lower graph shows the cumulative RMS of the spectra integrated from higher frequencies. The blue spectrum is measured when the SPI is turned off. The red one was measured with the SPI on. The total RMS of the blue spectrum is 3.8×10^{-7} m, and that of the red one is 4.2×10^{-8} m.

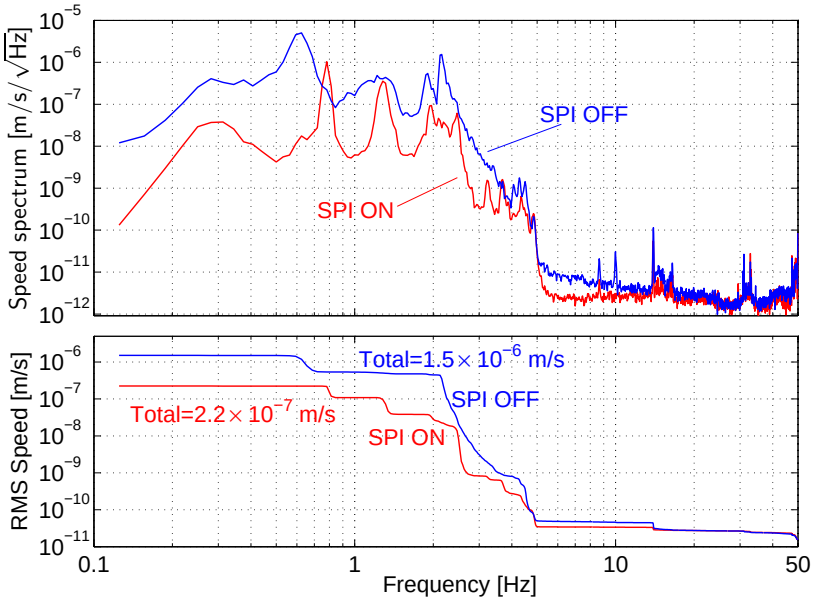

Fig. 6: The upper graph shows the speed spectra of the mirrors of the MIF. The lower part shows the cumulative RMSs of the speed spectra. The total RMS speed for the blue spectrum is 1.5×10^{-6} m/s, while it is 2.2×10^{-7} m/s for the red spectrum.

the noise was reduced by a factor of 10 to 100. In those frequencies coupling from vertical motion was the limiting factor. It is also important to note that because the two suspension systems are located close by (only 1.5 m away), there is already a significant common mode rejection effect at those low frequencies. Therefore, the noise reduction by the SPI was not as large as it would be in the case of a km scale interferometer, in which the ground motion is uncorrelated at both ends. Apart from some resonant peaks, the performance limiting factor at higher frequencies are coupling from other degrees of freedom (possibly pitch rotation) and laser frequency noise (above 5 Hz). The RMS displacement noise from 0.1 to 10 Hz was improved by a factor of 8 by the use of the SPI.

Fig.6 shows the noise spectra of the MIF in terms of the differential mirror speed. The RMS speed was reduced by a factor of 7.

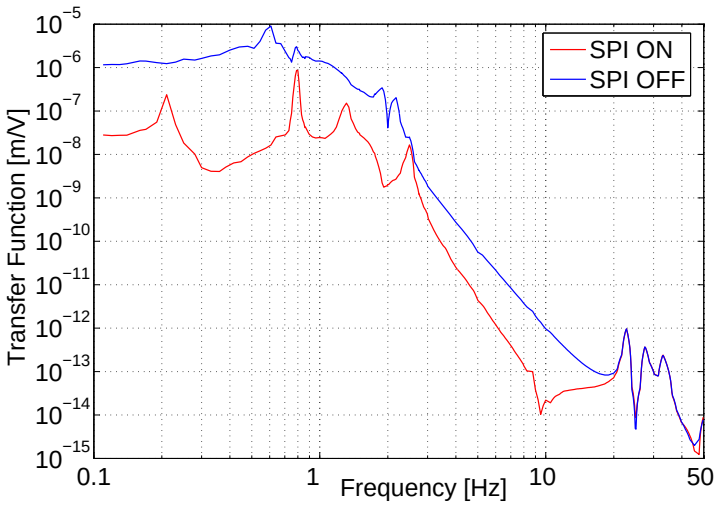

Fig. 7: Transfer functions from the input voltage of the horizontal actuator on the damping mass to the displacement of the MIF. The blue curve shows the transfer function when the SPI is off while the red one corresponds to the measurement with the SPI on.

Fig.7 shows the transfer functions measured from the damping mass (first stage) to the MIF. The coil-magnet actuators installed on the damping mass was used to excite the motion of the first stage. This measurement shows the potential performance of the SPI. The large peak in the red curve around 0.2 Hz is the vertical resonant frequency of the MGAS filters. Asymmetry of the excitation actuators induced the vertical motion around this frequency.

4 Advanced LIGO SPI

In this section I will discuss practical issues in implementing an SPI to Advanced LIGO.

4.1 Configuration

Location

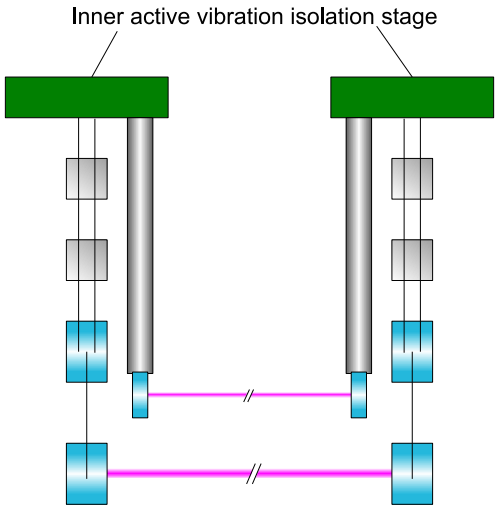

Fig. 8: Possible configuration of Advanced LIGO SPI with mirrors rigidly attached to the suspension platform by long arm.

In my experiment, the SPI was located one stage above the test masses. However in Advanced LIGO this is not practical because it requires significant modification to the quad-pendulum design. Moreover, the penultimate mass is not completely exposed to the beam tube (***confirmation needed***).

More plausible place to put SPI mirrors is the suspension platform from which the quad-suspension is hung. This configuration is conceptually shown in Fig.8. To bring the beam height down to the vacuum tube level, long rigid structures are used in the figure. However, this can introduce other problems. One is that the tilt of the platform is coupled to horizontal motion by this long leverage arm. Another worry is that the ISI might be incompatible with the large moment of inertia added by the long rigid structure. Resonances of the long rigid structure may also be a problem.

The distance from the suspension platform to the SPI's beam height is about 1 m. Therefore, to achieve $10^{-9}\mathrm{m}/\sqrt{\mathrm{Hz}}$ noise level, the tilt of the ISI platform must be below $10^{-9}\mathrm{rad}/\sqrt{\mathrm{Hz}}$, which is very difficult to achieve at low frequencies (~ 0.1 Hz).

To avoid those problems, Matt Evans suggested to use a suspended mirror for SPI as is shown in Fig.9. In this case, the mirror follows the motion of the platform at frequencies lower than its resonant frequency. However, above the resonant frequency, the SPI signal does not directly represent the motion of the platform. Still we could predict the motion of the platform from this sensor using the transfer function of the pendulum. The question here is how precisely we can do this.

If the transfer functions of the two SPI pendulums are different, the common motion of the suspension platform will leak into the SPI signal. This will be also a problem for this suspended mirror configuration.

Another idea to avoid the tilt problem is to use a suspended periscope to lower the beam height (Fig.10).

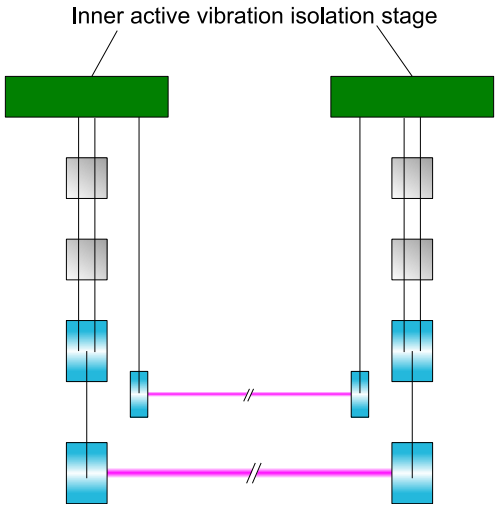

Fig. 9: SPI configuration with suspended mirrors.

With this configuration, we can effectively shorten the leverage arm length to the height of the mirror post in the first order approximation. We have to make the center of mass of the suspended periscope as close as possible to the point where the suspension wires are attached to prevent the rotation of the periscope by horizontal ground motion.

Above mentioned are just rough ideas and we need more detailed considerations.

Interferometer type

The required sensitivity for the SPI is not stringent (order of $10^{-9}\mathrm{m}/\sqrt{\mathrm{Hz}}$@0.1Hz. ***validation needed***) because our main target frequencies are around the micro-seismic peak (∼0.2 Hz) and the seismic motion there is large. To achieve this sensitivity, Fabry-Perot interferometer is probably not necessary. We can use an asymmetric Michelson interferometer as shown in Fig.11. We may even use corner cube reflectors as end mirrors for ease of alignment.

Another possibility is to use pseudo-random noise (PRN) heterodyne interferometry proposed by Daniel Shaddoc. This type of interferometer is planed to be used in LAI. According to the experimental results from the ANU group, this sensor can achieve nm level sensitivity.

Laser

The most strict requirement for the laser source comes to its frequency noise, because the SPI is directly sensitive to it regardless of whether the interferometer type is Fabry-Perot or asymmetric Michelson. The frequency noise of a free-run MISER would typically give $10^{-5}\mathrm{m}/\sqrt{\mathrm{Hz}}$ around 0.1 Hz. So we need a stabilized laser. Good quality laser light is available by picking up a fraction of the main laser. However this may introduce scattered light noise to the main interferometer because both the SPI and the MIF share the same vacuum tube. In this case, we have an option of turning off the SPI after the MIF is

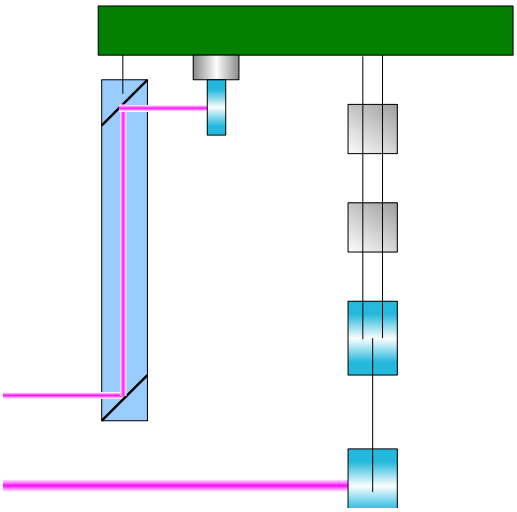

Fig. 10: Suspended periscope.

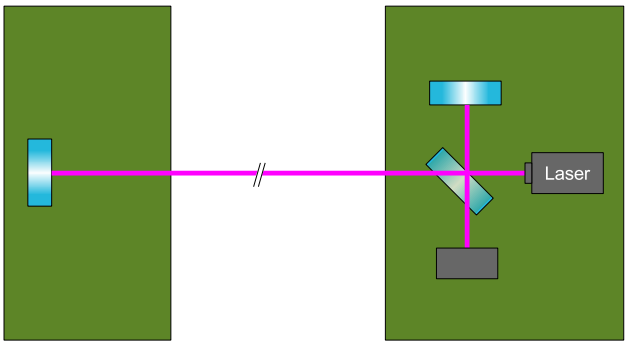

Fig. 11: Asymmetric Michelson interferometer
laser

locked because the SPI is mainly needed for the lock acquisition. Another solution may be shifting the frequency of the picked up main laser light by AOM or SHG. Then we can keep operating the SPI during the observation and the stability of the MIF may be improved.

The required laser power for the SPI is very small. Even for a Michelson interferometer locked at the middle of a fringe, which is the easiest to control but worst in shot noise, the required laser power to achieve the shot noise level of $10^{-10}\mathrm{m}/\sqrt{\mathrm{Hz}}$ is only 3 pW.

Control scheme

A difficulty lies in how to incorporate the control loop for the SPI into the existing active system control loop. The SPI servo must have enough gain (more than 100, preferably over 10000) at the frequencies of interest (around the micro seismic peak). To safely achieve this gain, the control bandwidth of about 10 Hz is desirable.

A possible feedback topology is to feed back the SPI signal only to one of the SPI stages (probably at the end station). The other stage is controlled only by the active loop. This means the active-only stage is anchored to the ground at DC with the relative position sensors. The dominant sensor for the SPI controlled stage is replaced from the sensors for the active isolation to the SPI in the beam direction. In this way, both of the SPI stages are ensured to be anchored to the ground at DC.

Now, how to integrate the SPI signal with the existing sensors of the active isolation system is an issue to be studied. A simple way is to add the SPI error signal to the error signal of the active isolation loop. However, this simple scheme may not work because of the finite gain and the phase delay of the active loop. Further study is needed for this issue.

4.2 Performance

As was discussed in Section 2, the performance of SPI depends mostly on the common mode rejection ratio (CMRR) of the suspension system below the SPI stage. Using a simple point-mass model of the quad-pendulum, the CMRR was calculated and shown in Fig.12. Here 1 mm of asymmetry in the pendulum length of each stage and 10 g of asymmetry in the mass of each stage are introduced.

The theoretical CMRR is very good as shown in Fig.12. However, there are several factors which can potentially limit the performance of the SPI. For example, the active damping applied at the top stage of the quad-pendulum may destroy the CMRR through asymmetry in the sensor gain, actuator gain etc...

Another possible limiting factor is coupling from other degrees of freedom. The SPI cannot suppress, for example, vertical motion of the SPI stages. A fraction of vertical motion is coupled to the main interferometer through mechanical imperfection of the suspension and ultimately the non-parallelism of local verticals at the ends. Once the dominant motion in the beam-direction is removed by the SPI, the buried contribution from the vertical motion may be exposed. Indeed, in my experiment, the low frequency noise reduction was limited by the coupling from vertical motion.

Estimation of those effects using the simulation model of the quad-pendulum is needed.

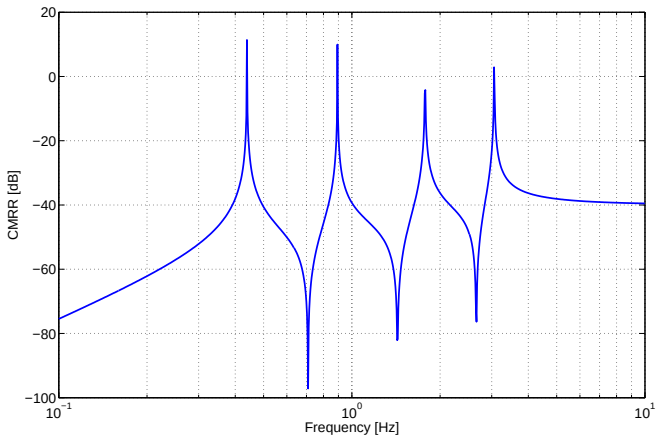

Fig. 12: CMRR of the quad-pendulum with 1 mm asymmetry in the length of each stage and 10 g asymmetry in the weight of each mass. Quality factors of the resonances are not properly taken into account in this model.

5 Future task list

5.1 Issues to be addressed

How to mount the SPI mirrors on the suspension platform

As was discussed in section 4.1, one of the biggest problem in the design of Advanced LIGO SPI is to find a proper way to mount the mirrors on the suspension platform. There are several preliminary ideas presented in section 4.1. However, more detailed analysis is needed.

If we use the suspended mirrors or periscope configurations, the CMRR of those suspended objects must be evaluated.

Decide optical configuration

We have to fix the optical configuration and parameters like, interferometer type (Michelson, Fabry-Perot or PRN), laser source (Independent laser or Picked up light with/without frequency shift etc...), laser power etc... Then we have to figure out an optical layout to fit in the BSC chamber without a significant change to the current design.

Evaluation of the CMRR of the quad-suspension

The common mode rejection and cross degrees of freedom coupling of the quad-suspension must be estimated by simulation. To do so, we have to introduce machining imperfections to the model by Monte Carlo and estimate the worst case performance. The impact of the active damping to the CMRR must also be simulated.

Integration of the SPI control loop with ISI

We have to decide a control topology and strategy to merge the SPI and the active isolation system. This requires thorough modeling of the systems, analysis and optimization of the control loops and validation of the scheme by simulation.

5.2 Experimental tests

Test of the quad-suspension for SPI

After the simulation of the quad-suspension, we may need to verify it with real measurements. A possible test is to hang two quad-suspensions from one stage and form a small Fabry-Perot interferometer between them. Then shake the common stage and measure the transfer function to the interferometer output. In this way we can measure the CMRR and coupling effect directly.

Test with an interferometer

At some point, it is necessary to test the SPI with an interferometer. The test has to be done in a facility with the advanced LIGO active vibration isolation system and quad-pendulum suspensions. One such a facility is LASTI. A major problem in doing this is that the LASTI arm consists of BSC and HAM chambers. So the cavity will be formed between a quad-sus and a triple-sus. This means poor CMRR is expected. However, we can still expect some CMRR at frequencies lower than the resonances of the suspensions. In addition, we can test the control scheme by feeding back the SPI signal only to the BSC.

5.3 Decision Tree

Here I present a preliminary decision tree to judge whether to use SPI in Advanced LIGO or not. This decision tree assumes that the SPI works fine. The issues to be addressed to evaluate the feasibility of AdvLIGO SPI are listed earlier in this section.

There are basically three main advantages in SPI. The first one is to help lock acquisition. However for this purpose, LAI looks more suitable. So if LAI works fine, SPI is not needed for this purpose. SPI can be regarded as a back up solution for LAI.

Secondly SPI can suppress the low-frequency seismic motion efficiently. Consequently the reduction of the burden to the actuators on the main mirrors will mitigate some technical problems like up-conversion noise, alignment fluctuation due to horizontal-pitch coupling and so on. This can also be achieved by the hierarchical control of the suspension system. If more suppression than what is provided by the hierarchical control is necessary, SPI can be used as an an additional vibration isolation mechanism. SPI could have a larger gain than hierarchical control because in the case of SPI, the sensing point and the actuation point are the same and the control scheme will be much simpler.

Finally, the SPI can in principle reduce the seismic noise of the main interferometer. The hierarchical control cannot reduce the displacement noise because it uses the same sensor for the measurement and the feedback. Since SPI is an independent sensor, the reduction of the seismic motion by SPI actually lower the seismic noise level seen by the main interferometer.

To reduce the seismic noise in the observation band (above 10 Hz), the SPI has to have a sufficient gain at those frequencies. Moreover, couplings from vertical and rotational degrees of freedom become more significant at higher frequencies in general. This is because those degrees of freedom are more difficult to isolate than the horizontal motion and consequently dominate the seismic noise spectrum at higher

frequencies. Therefore, SPI can reduce the seismic noise only in the frequency region where the seismic noise is still dominated by horizontal motion.

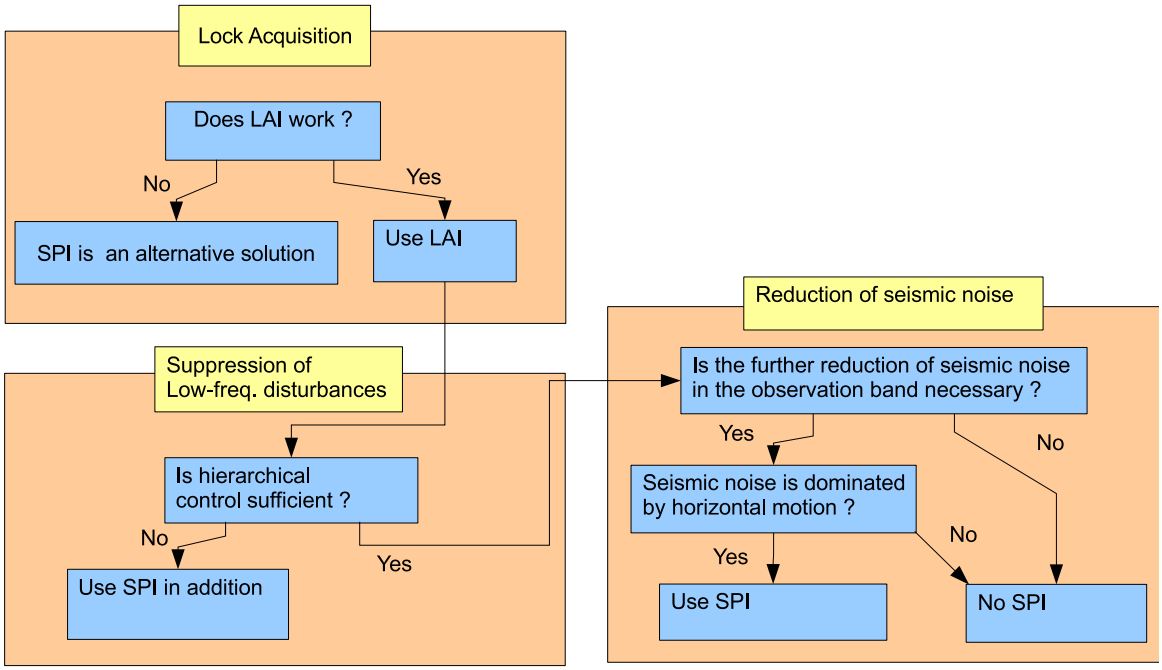

Fig. 13: Decision tree for Advanced LIGO SPI

References

[1] Osamu Miyakawa and Hiro Yamamoto, Personal communication

[2] Y. Aso, Master's thesis, University of Tokyo 2002, available from http://granite.phys.s.u-tokyo.ac.jp/theses/aso_m.pdf

[3] Y. Aso, M. Ando, K. Kawabe, S. Otsuka, K. Tsubono, *Phys. Lett. A*, **327** (1) 1-8, 2004

[4] Y. Aso, PhD thesis, University of Tokyo 2006, available from http://granite.phys.s.u-tokyo.ac.jp/theses/aso_d.pdf

[5] R.W.P. Drever, *LIGO Document* T870001-00-R (1987)

[6] R.W.P. Drever, S.J. Augst, *Classical Quant. Grav.*, **19** (2002) 2005.

[7] Glenn de Vine, David Rabeling, Bram Slagmolen, David McClelland, Daniel Shaddock, "Pseudo-random phase modulation for Adv LIGO lock acquisition", presentation available at http://ilog.ligo-wa.caltech.edu:7285/advligo/Seismic_Platform_Interferometer/SPI_Meetings_Telecons?action=AttachFile&do=get&target=ANU_SPI_LAI_PRNproposalv2_070822.pdf

[8] Daniel Shaddoc, "Digitally enhanced heterodyne interferometry", submitted to Optics Letters, 2007